

A Graphical Approach to NMR Experimental-Parameter Selection

T. A. EARLY, P. E. DONAHUE, AND E. A. WILLIAMS

GE Corporate Research & Development, One Research Circle, Niskayuna, New York 12309

Received December 16, 1996

The selection of acquisition parameters in a Fourier-transform NMR experiment should be based on the relaxation properties of the sample of interest and the desired qualities of the resulting spectrum, keeping in mind any experimental or technical constraints. In the unconstrained case where the spectroscopist has virtually full choice of both tip angle and repetition time, some of the trade-offs that can exist between sensitivity and integration accuracy have been discussed. The consequences of constraints on repetition time (1–4) or the desire for maximum integration accuracy (5, 6) have been shown. However, the interrelationships between tip angle, repetition time, integration accuracy, and accumulated signal-to-noise is not simple, and deciding on acquisition parameters for a typical, complex sample is not straightforward. When presented with a sample containing multiple resonances each with different relaxation properties, the choice of experimental parameters becomes more complex and the trade-off less obvious. This paper will illustrate graphically those relationships over a wide range of possible tip angles and repetition times as well as illustrate regions of this parameter space which are important to understand in terms of optimizing NMR acquisition conditions for a desired result, a given constraint, and/or complex sample requirement. In addition, the constraint of operating with a fixed tip angle will be discussed.

The Bloch equations describe the NMR relaxation process in terms of a simple, first-order kinetic process characterized by two relaxation times, T_1 and T_2 . T_1 , the longitudinal relaxation describes the behavior of magnetization parallel to the applied magnetic field while T_2 describes the behavior of magnetization perpendicular to the applied magnetic field. During any NMR experiment, the longitudinal magnetization is not at equilibrium, M_0 , but is repeatedly being perturbed by applying RF pulses at some repetition time, t , thus before the next pulse, some steady-state magnetization, M_{ss} is achieved, where $M_0 > M_{ss}$. Immediately after the pulse, longitudinal magnetization will be $M_{ss} \cos \theta$, where θ is the tip angle caused by the application of a short RF pulse. (We will ignore the effects of relaxation during the RF pulse and any off-resonance effects.) By simple conservation of magnetization, employing the Bloch equations, we have

$$M_{ss} = M_{ss} \cos \theta + (M_0 - M_{ss} \cos \theta)(1 - e^{-T}), \quad [1]$$

where T is a normalized repetition time, t/T_1 . Rearranging Eq. [1], we have

$$\frac{M_{ss}}{M_0} = \frac{1 - e^{-T}}{1 - \cos \theta e^{-T}} \equiv R. \quad [2]$$

This equation is important because it describes the completeness of magnetization recovery as a function of the pulse repetition time and pulse tip angle. This recovery directly relates to the accuracy of the accumulated signal intensity. For the purposes of this paper, we will call the quantity M_{ss}/M_0 , *recovery*, or R . The recovery is illustrated in Fig. 1 as a two-dimensional contour plot. It is observed from this figure and should also be intuitively obvious that more complete recovery is achieved with smaller tip angles and/or longer repeat times. For a multiple-acquisition experiment where R is important, the accumulated signal-to-noise is then proportional to

$$\frac{\sin \theta R}{\sqrt{T}}. \quad [3]$$

This relationship is shown in Fig. 2 and illustrates the relative accumulated signal-to-noise achievable in a given amount of time as a function of the two acquisition parameters, θ and T . The shape, or surface, of Eq. [3] has interesting features and characteristics which will be discussed further below, but for now it is of interest to consider the maximum, or ridge of the surface.

As pointed out by Ernst and Anderson (1), this surface has a maximum at any particular value of T and is described by the relationship

$$\cos \theta = e^{-T}. \quad [4]$$

It is important to reiterate that this equation describes the tip angle necessary to achieve the maximum sensitivity at some set repetition time and is the result of differentiating Eq. [3] with respect to θ and setting the resulting equation to zero. Equation [4] defines the Ernst angle and is shown as the dotted curve in Fig. 2.

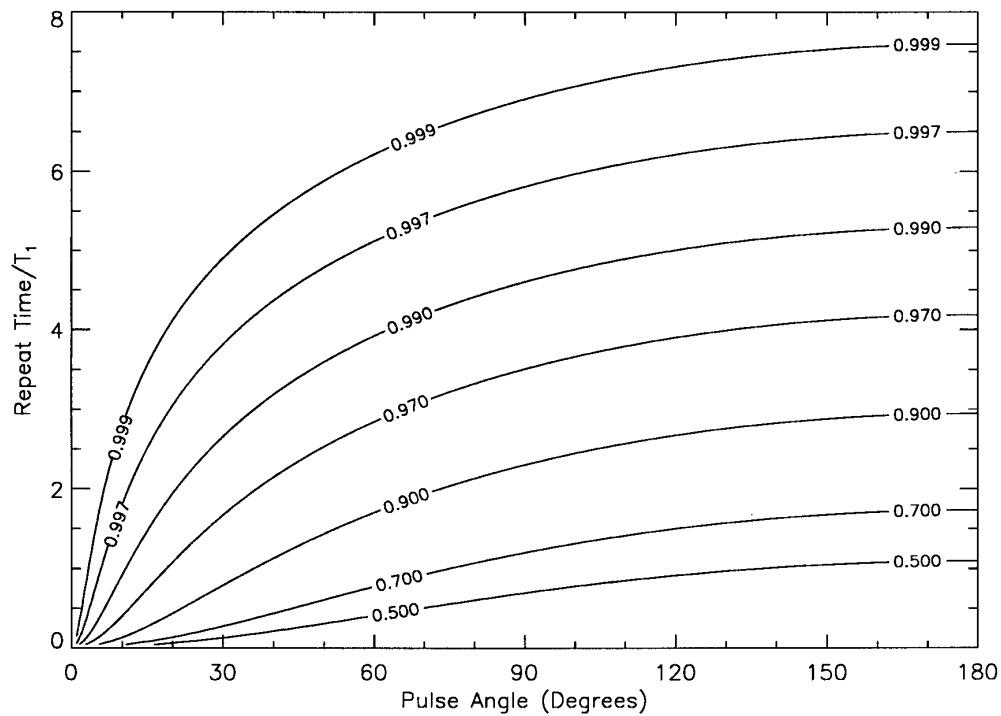


FIG. 1. This isocontour plot is of the steady-state fraction of magnetization recovery (Eq. [2]) as a function of the pulse angle, in degrees, and the pulse repetition time, in units of the T_1 relaxation time. Each isocontour is labeled with its magnetization recovery fractional value.

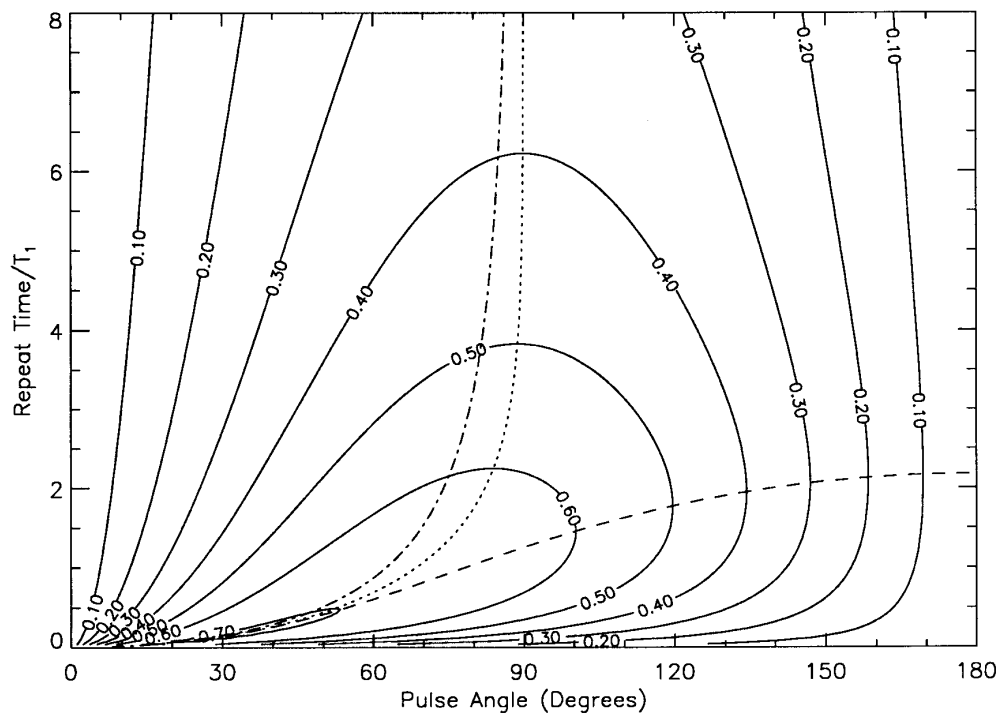


FIG. 2. This isocontour plot is of the relative signal-to-noise per unit time (Eq. [3]) as a function of the pulse angle, in degrees, and the pulse repetition time, in units of the T_1 relaxation time. Each isocontour is labeled with its value.

Traficante (6) later showed that in order to achieve a given accuracy (or recovery), slightly different acquisition parameters are required. These optimum parameters may be determined graphically by overlaying Figs. 1 and 2, traveling along the desired R isocontour of Fig. 1 until a maximum is reached in Fig. 2. It can be shown that the relationship between θ and T for any value of R is

$$\cos \theta = R \left(\frac{\sin^2 \theta}{2T} + \cos^2 \theta \right). \quad [5]$$

This relationship is shown in Fig. 2 as the dot-dash curve. Comparing equivalent R -value conditions for these two curves will show that slightly better accumulated signal-to-noise per unit time will result if acquisition parameters are selected from Eq. [5] rather than Eq. [4]. A maximum accumulated signal-to-noise per unit time improvement of about 1% is found at $R \approx 0.9$ with less improvement at other values of R .

Finally, another important feature of Fig. 2 is the maximum sensitivity at any given θ . This can be obtained analytically by equating with zero the derivative of Eq. [3] with respect to θ . This maximum is plotted as the dashed curve in Fig. 2 and is described by

$$\cos \theta = \frac{e^T - 2T - 1}{1 - 2T + e^{-T}}. \quad [6]$$

This curve describes the optimum repetition time for any given tip angle and is particularly important at $\theta = 90^\circ$ where $T \approx 1.25$. This is because a number of experiments demand, for the sake of efficiency, 90° tip angles. A good example of the kinds of experiments which can benefit from this optimization are the Hahn spin-echo experiment and the Hartman-Hahn solids cross-polarization experiment. These two experiments represent the most popular forms of NMR imaging and the NMR of solids.

Figure 2 shows the result that maximum signal-to-noise efficiency is achieved at a relatively small region of param-

eter space near very short repetition time and reasonably small tip angles. However, as pointed out by Waugh (2), these conditions may not be achievable in most situations due to constraints in the data-acquisition time. That is, the acquisition time should be at least several T_2^* values, the FID decay time. When $T_1 \approx T_2 \approx T_2^*$, as in the case of small molecules in solution, the fastest achievable repetition times are limited by the FID decay rate.

In the case where $T_1 \gg T_2^*$, typical of macromolecular solutions and solids, it may be possible to access this area of parameter space. Other problems might arise however. In particular, if there is an interest in multiple resonances with different T_1 values, it may be possible to adjust acquisition parameters for one resonance for maximum sensitivity while, due to the steepness of the drop-off around the maximum of Eq. [3], other resonances suffer great losses in sensitivity. For this reason, it may be much more beneficial to operate around $R \approx 2$ and $\theta \approx 80^\circ$. R can be chosen to be the approximate average for each of T_1 values of interest. With these acquisition parameters, even resonances with T_1 values furthest from the average will still be in a reasonable position of sensitivity.

The two-dimensional graphs presented here show both magnetization recovery and accumulated signal-to-noise per unit time as a function of both pulse repetition time and pulse tip angle. These figures can provide the spectroscopist with both a qualitative feel and a quantitative estimate of the sensitivity and accuracy of a given sample and experiment conditions. In those situations where the tip angle is constrained, Fig. 2 can be used to estimate the proper repetition time for optimum sensitivity.

REFERENCES

1. R. R. Ernst and W. A. Anderson, *Rev. Sci. Instrum.* **37**, 93 (1966).
2. J. S. Waugh, *J. Mol. Spectrosc.* **35**, 298 (1970).
3. E. D. Becker, J. A. Ferretti, and R. N. Gambhir, *Anal. Chem.* **51**, 1413 (1979).
4. R. Dupree and M. E. Smith, *J. Magn. Reson.* **75**, 153 (1987).
5. D. J. Cookson and B. E. Smith, *Anal. Chem.* **54**, 2591 (1982).
6. D. D. Traficante, *Concepts Magn. Reson.* **4**, 153 (1992).